ELSEVIER

SCIENCE DIRECT®

PHYSICS LETTERS B

Physics Letters B 579 (2004) 265–270

www.elsevier.com/locate/physletb

# E1 strength of the subthreshold $3/2^+$ state in $^{15}$O studied by Coulomb excitation

K. Yamada [a], T. Motobayashi [b], H. Akiyoshi [b], N. Aoi [b], Zs. Fülöp [d], T. Gomi [a], Y. Higurashi [b], N. Imai [b], N. Iwasa [e], H. Iwasaki [c], Y. Iwata [g], H. Kobayashi [a], M. Kurokawa [b], Z. Liu [h], T. Minemura [b], S. Ozawa [b], H. Sakurai [c], M. Serata [a], S. Shimoura [f], S. Takeuchi [b], T. Teranishi [f], Y. Yanagisawa [b], K. Yoshida [b], M. Ishihara [b]

[a] *Department of Physics, Rikkyo University, Toshima, Tokyo 171-8501, Japan*
[b] *The Institute of Physical and Chemical Research (RIKEN), Wako, Saitama 351-0198, Japan*
[c] *Department of Physics, University of Tokyo, Bunkyo, Tokyo 113-0033, Japan*
[d] *Institute of Nuclear Research of the Hungarian Academy of Sciences, PO Box 51, 4001 Debrecen, Hungary*
[e] *Department of Physics, Tohoku University, Aoba, Sendai, Miyagi 980-8578, Japan*
[f] *Center for Nuclear Study (CNS), University of Tokyo, RIKEN Campus, Wako, Saitama 351-0198, Japan*
[g] *National Institute of Radiological Sciences, Inage, Chiba 263-8555, Japan*
[h] *Institute of Modern Physics, Chinese Academy of Sciences, Lanzhou, 730000, PR China*

Received 7 July 2003; received in revised form 11 October 2003; accepted 11 November 2003

Editor: J.P. Schiffer

**Abstract**

The radiative width of the $3/2^+$ state at 6.793 MeV in $^{15}$O has been experimentally determined to be $\Gamma_\gamma = 0.95^{+0.60}_{-0.95}$ eV by intermediate-energy Coulomb excitation. Our result independently supports the recent studies which point to a minor contribution of this state to the astrophysical rate of the $^{14}$N(p,$\gamma$)$^{15}$O reaction in the CNO-cycle hydrogen burning in massive stars.



*PACS:* 23.20.Js; 25.40.Lw; 25.60.-t; 25.70.De; 26.20.+f

*Keywords:* Coulomb excitation; CNO cycle; Radiative width; Radioactive beam

The $^{14}$N(p,$\gamma$)$^{15}$O reaction at low energies has attracted much interest in regards to nuclear astrophysics [1,2]. This reaction is particularly essential in the hydrogen-burning stage of a massive main-sequence star as this reaction, being the slowest in the main CNO cycle in stellar conditions, dominates the rate of energy generation through the entire cycle [1]. This reaction also contributes to the rate of solar hydrogen burning processes [3]. So far, several experiments have been made of the $^{14}$N(p,$\gamma$)$^{15}$O reaction at $E_p > 100$ keV, either by measuring $\beta^+$ activity of the residual $^{15}$O nucleus [4–6], or by observing prompt

*E-mail address:* nari@ne.rikkyo.ac.jp (K. Yamada).

0370-2693 
doi:10.1016/j.physletb.2003.11.024

capture $\gamma$-transitions [7–10]. Recently, an attempt was made to extract the $^{14}$N(p,$\gamma$)$^{15}$O reaction cross sections at lower energies from the transfer reaction of $^{14}$N(d,n)$^{15}$O through the measurement of the asymptotic normalization coefficient for $^{15}$O [11].

The behavior of the low-energy (p,$\gamma$) capture yield is influenced by the tails of a few discrete levels [2,10]. Among them, the s-wave resonance located 504 keV below the p + $^{14}$N threshold, which corresponds to the $3/2^+$ state at 6.793 MeV excitation energy in $^{15}$O, has attracted much attention [3,10]. Schröder et al. extracted the radiative width of the $3/2^+$ state to be $\Gamma_\gamma = 6.3$ eV by an R-matrix fit to their experimental excitation function [10]. This width is much larger than other evaluations. Assuming isospin symmetry with the 7.301 MeV $3/2^+$ analog state in $^{15}$N, $\Gamma_\gamma = 1.08 \pm 0.08$ eV [12], we obtain a $\Gamma_\gamma = 0.87$ eV for the 6.793 MeV state in $^{15}$O. A recent R-matrix analysis by Angulo and Descouvemont gives the width $\Gamma_\gamma = 1.75 \pm 0.60$ eV [13], based on the same data as those used in Ref. [10]. These widths of 0.87 eV and 1.75 eV lead to negligible contribution of the $3/2^+$ state to the $^{14}$N(p,$\gamma$)$^{15}$O reaction rate, while the width of 6.3 eV increases the astrophysical $S$-factor at zero energy by about 50% compared with the one estimated without any resonance effect. Here, the $S$-factor is defined as $S = \sigma E \exp(2\pi\eta)$ with the Sommerfeld parameter $\eta = e^2 Z_1 Z_2/\hbar v$ [14]. A recent lifetime measurement using the Doppler-shift attenuation method reported the mean life of $1.60^{+0.75}_{-0.72}$ fs for the $3/2^+$ state in $^{15}$O [15], which corresponds to a width $\Gamma_\gamma = 0.41^{+0.34}_{-0.13}$ eV, suggesting again negligible contribution of the $3/2^+$ state to the $^{14}$N(p,$\gamma$)$^{15}$O reaction rate.

The present article reports on a measurement of the radiative width for the $3/2^+$ state at 6.793 MeV in $^{15}$O by intermediate-energy Coulomb excitation using inverse kinematics [16,17]. Energies, angular distributions, and $\gamma$-yields from de-excitation $\gamma$-rays from fast-moving ejectiles are measured with Doppler-shift correction. For E1 transitions, inelastic cross sections are almost free from the nuclear-excitation contribution even for light nuclei as in the present case [18–20]. Since this method is independent of the ones employed in the earlier experiments [4–11,15], the present study is expected to provide complementary information and help resolve the conflicting situation mentioned above.

The experiment was performed at the RIKEN Accelerator Research Facility. An $^{15}$O beam was produced by using the projectile fragmentation of a 135 $A$ MeV $^{16}$O beam incident on a 740 mg/cm$^2$ thick $^9$Be target, and was isotopically separated by the RIKEN Projectile-fragment Separator (RIPS) [21]. To prevent $\gamma$-ray background caused by primary $^{16}$O beam interactions downstream of the RIPS primary target, a swinger magnet directly upstream of the primary target offset the primary $^{16}$O beam by 4 degrees with respect to the central axis of the RIPS system. This method stopped the primary $^{16}$O beam in a heavily shielded area just after the primary target. The typical $^{15}$O intensity was about $4 \times 10^5$ counts per second, and the energy was 100 $A$ MeV with an energy spread of about 2.5%. The isotopic purity of $^{15}$O in the secondary beam was approximately 64%, and major contamination was $^{14}$N, which was able to be rejected by the time-of-flight TOF measurement. The beam was focused onto a lead target of 1480 mg/cm$^2$ thickness placed at the final focal plane (F3) of RIPS. The average energy in the middle of the lead target was about 85 $A$ MeV. Identification of $^{15}$O in the secondary beam was carried out event-by-event by measuring the (TOF) using a 1.0 mm thick plastic scintillator installed at the second focal plane (F2) of RIPS and cyclotron RF signals.

In order to detect and identify reaction particles, a plastic scintillator hodoscope [22,23] of a $1 \times 1$ m$^2$ active area consisting of a 5 mm thick $\Delta E$ plane and a 60 mm thick $E$ plane was placed in vacuum 5.0 m downstream from the lead target. Isotopic identification of the particles was performed by measuring the energies deposited in the $\Delta E$ and $E$ hodoscope detectors and the TOF between the F2 plastic scintillator and the hodoscope. It was found that $^{15}$O was clearly separated from other oxygen isotopes. For E1 Coulomb excitation, 90% of the inelastically scattered $^{15}$O particles were detected by the hodoscope. In evaluating this value, loss of events due to nuclear reactions in the detector material as well as the detector solid angle were taken into account. More details of the hodoscope are described in Refs. [22,23].

A NaI(Tl) array (DALI) placed around the lead target was used to detect de-excitation $\gamma$-rays from scattered $^{15}$O particles. As shown in Fig. 1, DALI consisted of sixty-four NaI(Tl) scintillators and each

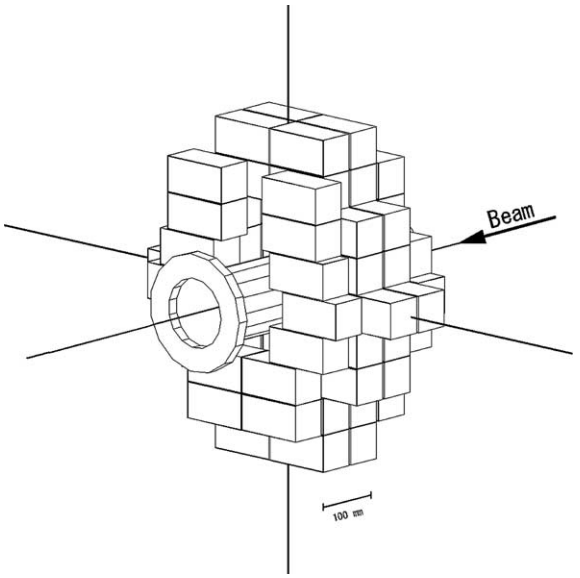


Fig. 1. A schematic view of the DALI array, with sixty-four NaI(Tl) scintillators. The intersection of the three straight lines penetrating the array indicate the target center.

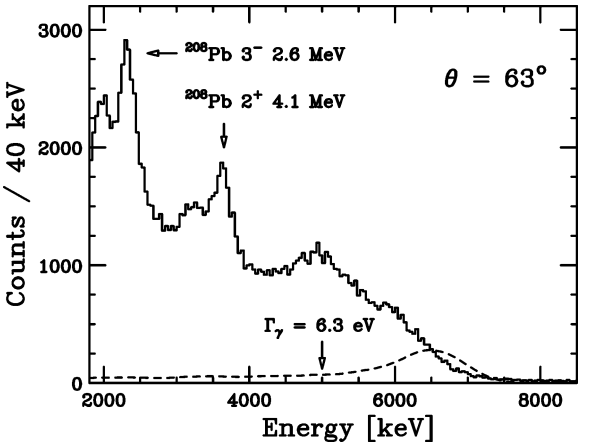


Fig. 2. Energy spectrum of $\gamma$-rays measured at 63 degrees obtained for the $^{15}\mathrm{O} + \mathrm{Pb}$ inelastic scattering. The spectrum is Doppler-shift corrected to be in the rest frame of $^{15}$O. The expected spectrum for the $3/2^+ \rightarrow 1/2^-_{\mathrm{g.s.}}$ transition with $\Gamma_\gamma = 6.3$ eV is shown by the dashed curve. (See text for details.)

scintillator crystal was of $6 \times 6 \times 12$ cm$^3$ volume. The scintillators were arranged to form four layers, and the average angles of the layers were 63, 86, 105, and 127 degrees, respectively, with respect to the beam direction. The Doppler shift was corrected for event-by-event using the $\gamma$-ray emission angle determined with an accuracy of about 20 degrees (FWHM). The spread in the direction of the scattered $^{15}$O was neglected, since the particles were measured only at forward angles up to about 6 degrees. The detectors at 63 degrees were mainly used for measuring $\gamma$-rays from $^{15}$O, while the detectors at 127 degrees were used for estimating the $\gamma$-ray yield due to target excitation, the details of which will be described later. The absolute efficiency and line shape of $\gamma$-ray energy spectra were simulated using the GEANT Monte Carlo code [24]. The calculated efficiency of the fourteen detectors at 63 degrees was 5% for 6.793 MeV $\gamma$-rays from $^{15}$O nuclei in flight with a relativistic velocity $\beta = 0.40$.

Since the energy of the $\gamma$-rays measured in the present experiment is high (around 7 MeV), the energy deposited is usually spread over several detectors, mainly through electron–positron pair creation. Hence, the $\gamma$-ray energy spectra are constructed by adding up the energy deposited in a "cluster" of crystals. The size of the cluster was chosen so as to achieve a high full-energy-peak efficiency with a reasonably low probability of including two independent $\gamma$-rays. Based on the GEANT calculation, we adopted a 15 cm radius between crystal centers as the definition of a cluster. Among the crystals in a cluster, the one having the largest energy deposition was assigned to the detector of the first $\gamma$-interaction, and the angle of the first detector was used for the Doppler correction. The probability of a misassignment of the first hit was calculated by the Monte Carlo simulation, and was taken into account in calculating the line shapes described shortly.

Fig. 2 shows the Doppler-corrected energy spectrum of $\gamma$-rays measured in coincidence with scattered $^{15}$O by the array detectors placed at 63 degrees. As indicated by the arrows in Fig. 2, two $\gamma$-ray peaks associated with excitation of the target nucleus $^{208}$Pb were also observed at 2.3 MeV and 3.6 MeV, which correspond to the $\gamma$-decays from the 2.6 MeV $3^-$ state and 4.1 MeV $2^+$ state, respectively. The energy shifts are due to the Doppler correction for moving $\gamma$-emitters with $\beta = 0.40$. In order to avoid admixture of the target excitation components into the energy region of the $\gamma$-rays in $^{15}$O, only the $\gamma$-ray yields obtained from the set of detectors placed at 63 degrees, the most forward angle in the present $\gamma$-ray detector setup, were used.

For the 63 degree detectors, the 6.793 MeV $\gamma$-rays from the $3/2^+$ state in $^{15}$O, our focus in the present experiment, are shifted up to 7.61 MeV in the laboratory flame, where essentially no $\gamma$-ray from $^{208}$Pb is expected.

As one can see in Fig. 2, no distinct peak is observed at energies around 6.793 MeV, the energy of the $3/2^+ \to 1/2^-_{\mathrm{g.s.}}$ transition in $^{15}$O. The dashed curve in the figure represents the peak shape calculated from the radiative width $\Gamma_\gamma = 6.3$ eV evaluated by Schröder et al. [10]. This line shape was obtained by a Monte Carlo calculation, in which the "cluster method" described above was simulated. The beam spot size, energy losses in the target, energy resolution and efficiency of the detectors, and Doppler effects were also taken into account. It should be noted that the single- and double-escape peaks overlap with the full-energy peak due to the large Doppler broadening. The E1 Coulomb excitation cross section was calculated by the coupled-channel code ECIS97 [25]. As clearly seen in Fig. 2, the choice of width 6.3 eV is too large to be consistent with the present experimental data.

In order to extract more quantitative information on $\Gamma_\gamma$, the spectrum obtained by the 63 degree detectors was analyzed with the following six components: four line-shapes from the transitions in $^{15}$O (5.241 MeV ($5/2^+ \to 1/2^-_{\mathrm{g.s.}}$), 6.176 MeV ($3/2^- \to 1/2^-_{\mathrm{g.s.}}$), 6.793 MeV ($3/2^+ \to 1/2^-_{\mathrm{g.s.}}$), and 7.276 MeV ($7/2^+ \to 1/2^-_{\mathrm{g.s.}}$)) obtained by the Monte Carlo calculation; a target excitation component, and a continuous background component. It should be noted that the 5.183 MeV line due to the ground state transition from $1/2^+$ state in $^{15}$O was included in the 5.241 MeV component by neglecting their small energy-difference. The target excitation component was determined from the energy spectrum obtained by the backward angle array detectors at 127 degrees. The energies of photons from the excited $^{15}$O nuclei were greatly reduced by the Doppler effect at 127 degrees. The backward emitted $\gamma$-ray from the $^{15}$O was shifted to energies lower than 5 MeV in the laboratory frame, which corresponds to 4.5 MeV in the Doppler-corrected spectrum at 63 degrees. Hence, the yield above 5 MeV in the 127 degree spectrum is dominated by the $\gamma$-rays from the target. In addition, the backward $\gamma$-ray yield from $^{15}$O was found experimentally to be much smaller than the yield due to the target excitation in the same energy region. The shape of the continuous background component was assumed to be an exponential function. The amplitude of the 5.241 MeV-, 6.176 MeV-, and 6.793 MeV-transitions in $^{15}$O; the magnitude of the target excitation; and the slope and amplitude of the exponential background were treated as fitting parameters. The slope of the exponential background was mainly determined by the $\gamma$-ray spectrum above 8 MeV. Its uncertainty was estimated to be 60% by changing the region of the fits, which led to the 20% error for the $\gamma$-ray yield of the 6.793 MeV transition. In the fit, the amplitude for the 7.276 MeV transition was fixed to the value evaluated from the lifetime and branching ratio by distorted-wave calculations discussed later. Ambiguities in the lifetime and branching ratio of the 7.276 MeV state were taken into account in estimating errors in the fitting results together with the one for the slope of the exponential background.

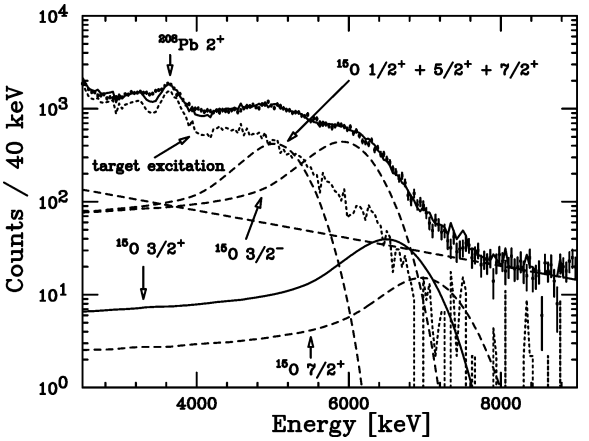


Fig. 3. Fits of the Doppler-corrected $\gamma$-spectrum from Coulomb excitation of $^{15}$O. The experimental data for the $^{15}$O + Pb inelastic scattering measured at 63 degrees are plotted with their $1\sigma$ error bars. The curves show the results of the best fits of the six components: four spectra due to the $^{15}$O excitation, target excitation component, background component. The total sum is shown by the solid curve through the data points. (See text for details.)

The result of the fit is shown by the solid curve in Fig. 3 together with the individual contributions of the other six components. The data are well reproduced by the sum of the six components. From the fit, the resulting cross sections are found to be $4.3 \pm 0.9$, $5.3 \pm 1.1$, and $0.55 \pm 0.35$ mb for the 5.2, 6.2, and 6.8 MeV components, respectively. The detection efficiencies for $\gamma$-

ray and scattered-particle measurements were taken into account in deducing the above cross sections. The errors include the ambiguities associated with the present fitting procedure, and the common systematic uncertainties in the detection efficiency (12%), the beam intensity (7%), particle identification (10%), distorted-wave calculation (5%), and the $\gamma$-ray angular distribution (5%). The radiative width for the $3/2^+$ state, $\Gamma_\gamma = 0.95 \pm 0.60$ eV, was derived from the cross section for the 6.8 MeV component with the help of a distorted-wave calculation assuming pure E1 Coulomb excitation. The optical potential parameters were taken from Ref. [26], where the data of the $^{17}\mathrm{O} + {}^{208}\mathrm{Pb}$ scattering at 84 $A$ MeV were analyzed to obtain the potential. Note that the Coulomb excitation method determines the partial width corresponding to the $\gamma$-decay to the ground state. In the present case, however, the radiative width is directly obtained from the Coulomb excitation cross section, because the $3/2^+$ state is known to decay to the ground state in 100% probability. Since the effects of nuclear excitation are expected to be very small as mentioned earlier, uncertainties regarding the nuclear component are not included in the error. Contributions from other $\gamma$-transitions feeding the 6.8 MeV state could cause the $\Gamma_\gamma = 0.95 \pm 0.60$ eV value to be smaller than determined. Because the $1\sigma$ upper bound cannot be made smaller by feeding, it is appropriate to provide an experimental radiative width of $0.95^{+0.60}_{-0.95}$ eV. This result is compatible with the recent lifetime measurement that gives the width of $0.41^{+0.34}_{-0.13}$ eV [15], while the higher value of 6.3 eV reported in the R-matrix analysis of $^{14}\mathrm{N(p,}\gamma)^{15}\mathrm{O}$ data [10] is excluded. A new analysis on the same (p,$\gamma$) data of Ref. [10] predicts the width of $1.75 \pm 0.60$ eV [13], and the present result is almost compatible with this new analysis. The small radiative width below 2 eV is expected to give only a minor effect of the $3/2^+$ state on the low-energy $^{14}\mathrm{N(p,}\gamma)^{15}\mathrm{O}$ cross section which is of importance in the CNO-cycle hydrogen burning.

To examine the results for the 5.2 and 6.2 MeV components, their cross sections were compared with estimates based on distorted-wave calculations with known spectroscopic information. We assumed the angular momentum transfer $\ell$ to be the lowest possible value, i.e., $\ell = 1$ for $1/2^+$ excitation, $\ell = 2$ for $3/2^-$, and $\ell = 3$ for $5/2^+$ and $7/2^+$. Both the Coulomb (E$\ell$) and nuclear excitations were included except for $\ell = 1$ where only E1 Coulomb excitation was taken into account. Magnetic excitation processes were neglected because of their small inelastic cross sections. The nuclear excitation amplitudes were calculated with the collective deformation model. The probabilities of the $\gamma$-decay transitions were taken from Ref. [27]. Referring to Fig. 3, the first peak at 5.2 MeV is expected to be formed by the direct excitation to the $^{15}\mathrm{O}$ $1/2^+$ state at 5.183 MeV and $5/2^+$ state at 5.241 MeV, while the excitation to the higher state ($7/2^+$ at 7.276 MeV) also contributes by the cascade $\gamma$-decay via the 5.241 MeV $5/2^+$ state. The sum of the estimated cross sections for the $1/2^+$, $5/2^+$, and $7/2^+$ states (0.08, 2.4, and 5.4 mb, respectively) amounts to $8 \pm 5$ mb. The contributions to the error come from those of the half lives (45%), optical potential dependence of the calculated nuclear excitation cross sections (30%), and possible difference between the nuclear and Coulomb deformations (20%). The present result of $4.3 \pm 0.9$ mb for the two states near 5.2 MeV is consistent with this estimation. For the second peak at 6.2 MeV, only an upper limit (1.74 fs) is known for the half life of $3/2^-$ state at 6.176 MeV, which leads to the lower limit of the inelastic cross section of 0.31 mb. The value from the present study, $5.3 \pm 1.1$ mb, is larger by an order of magnitude than the quoted lower-limit, implying a lifetime shorter by an order of magnitude.

We have studied experimentally the Coulomb excitation of $^{15}\mathrm{O}$ to its $3/2^+$ state at the excitation energy of 6.793 MeV, which was expected to affect the low-energy $^{14}\mathrm{N(p,}\gamma)^{15}\mathrm{O}$ reaction, a key reaction of the CNO cycle in massive stars. A radioactive $^{15}\mathrm{O}$ beam bombarded a lead target at 85 $A$ MeV average energy, and de-excitation $\gamma$-rays were measured in coincidence with inelastically scattered $^{15}\mathrm{O}$ particles. A radiative width of the $3/2^+$ state was extracted to be $\Gamma_\gamma = 0.95^{+0.60}_{-0.95}$ eV. The present result provides independent support to other recent studies that give small $\Gamma_\gamma$ values, $0.41^{+0.34}_{-0.13}$ eV [15], and $1.75 \pm 0.60$ eV [13]. However, the prediction of 6.3 eV by Schröder et al. [10] is not compatible with the present Coulomb excitation result. This suggests that the role of the $3/2^+$ subthreshold state is considerably small and negligible for the low-energy $^{14}\mathrm{N(p,}\gamma)^{15}\mathrm{O}$ cross section, and possible increase of the $S$-factor toward zero energy is not favorable in contrast to the prediction in Ref. [10].

## Acknowledgements

The authors thank the RIKEN Ring Cyclotron staff members for their help during the experiment. This work was supported by the Grant-in-Aid for Scientific Research under the program number 10304021 from the Ministry of Education, Culture, Sports, Science and Technology.

## References

[1] C. Rolfs, H.P. Trautvetter, W.S. Rodney, Rep. Prog. Phys. 50 (1987) 233.
[2] M. El Eid, et al., in: N. Prantzos, S. Harissopoulos (Eds.), Proceedings of Nuclei in the Cosmos V, Editions Frontières, Paris, 1999, p. 123.
[3] E.G. Adelberger, et al., Rev. Mod. Phys. 70 (1998) 1265.
[4] E.J. Woodbury, et al., Phys. Rev. 75 (1949) 1462.
[5] D.B. Duncan, et al., Phys. Rev. 82 (1951) 809.
[6] W.A.S. Lamb, R.E. Hester, Phys. Rev. 108 (1957) 1304.
[7] R.E. Pixley, PhD Thesis, California Institute of Technology, 1957.
[8] G.M. Bailey, D.F. Hebbard, Nucl. Phys. 46 (1963) 529; G.M. Bailey, D.F. Hebbard, Nucl. Phys. 49 (1963) 666.
[9] H.W. Becker, et al., Z. Phys. A 305 (1982) 319.
[10] U. Schröder, et al., Nucl. Phys. A 467 (1987) 240.
[11] P.F. Bertone, et al., Phys. Rev. C 66 (2002) 055804.
[12] R. Moreh, et al., Phys. Rev. C 23 (1981) 988.
[13] C. Angulo, P. Descouvemont, Nucl. Phys. A 690 (2001) 755.
[14] W.A. Fowler, G.R. Caughlan, B.A. Zimmerman, Annu. Rev. Astron. Astrophys. 5 (1967) 525.
[15] P.F. Bertone, et al., Phys. Rev. Lett. 87 (2001) 152501.
[16] T. Motobayashi, et al., Phys. Lett. B 346 (1995) 9.
[17] T. Glasmacher, Annu. Rev. Nucl. Part. Sci. 48 (1998) 1.
[18] C.A. Bertulani, Phys. Rev. C 49 (1994) 2688.
[19] H. Iwasaki, et al., Phys. Lett. B 491 (2000) 8.
[20] T. Motobayashi, Nucl. Phys. A 693 (2001) 258.
[21] T. Kubo, et al., Nucl. Instrum. Methods B 70 (1992) 309.
[22] I. Hisanaga, et al., RIKEN Accel. Prog. Rep. 31 (1998) 162.
[23] H. Iwasaki, et al., Phys. Lett. B 481 (2000) 7.
[24] GEANT3: Detector Description and Simulation Tool, CERN, Geneva, 1993.
[25] J. Raynal, Coupled channel code ECIS97, unpublished.
[26] J. Barrette, et al., Phys. Lett. B 209 (1988) 182.
[27] F. Ajzenberg-Selove, Nucl. Phys. A 525 (1991) 1.